On the Performance of SSK Modulation over Multiple–Access Rayleigh Fading Channels

Marco Di Renzo
L2S, UMR 8506 CNRS – SUPELEC – Univ Paris–Sud
Laboratory of Signals and Systems (L2S)
French National Center for Scientific Research (CNRS)
École Supérieure d'Électricité (SUPÉLEC)
University of Paris–Sud XI (UPS)
3 rue Joliot–Curie, 91192 Gif–sur–Yvette (Paris), France
E–Mail: marco.direnzo@lss.supelec.fr

Harald Haas
The University of Edinburgh
College of Science and Engineering
School of Engineering
Institute for Digital Communications (IDCOM)
Alexander Graham Bell Building, King's Buildings
Mayfield Road, Edinburgh, EH9 3JL, UK
E–Mail: h.haas@ed.ac.uk

***Abstract*— Spatial Modulation (SM) is a recently proposed joint coding and modulation scheme for Multiple–Input–Multiple–Output (MIMO) wireless systems, which is receiving a growing interest. SM offers a low–complexity alternative to the design of MIMO wireless systems, which avoids multiple Radio Frequency (RF) chains at the transmitter and high–complexity interference cancelation algorithms at the receiver, but still guarantees a multiplexing gain that only depends on the number of antennas at the transmitter. This makes this technology especially suitable for the downlink with low–complexity mobile units. So far, the feasibility and performance of SM have been assessed and studied only for point–to–point communication systems, *i.e.*, the single–user scenario. However, the performance achievable by the vast majority of wireless communication networks is interference limited, due to the simultaneous transmission of various users over the same physical wireless channel. Therefore, the adoption of SM in the next generation of wireless communication systems requires a deep understanding of its performance over interference channels. Motivated by this consideration, in this paper we study the performance of SM over the reference multiple–access fading channel composed by two transmitters and one receiver. Two detectors at the receiver are studied, *i.e.*, the single– and the multi–user detector. In particular, analysis and Monte Carlo simulations show that the single–user detector does not offer, in general, good error performance for arbitrary channel conditions, while the multi–user detector achieves error performance very close to the single–user lower–bound. These results clearly highlight that SM can be adopted for enabling data transmission over multiple–access fading channels as well.**

I. Introduction

Multiple–antenna techniques constitute a key technology for modern wireless communications, which trade–off better error performance and higher data rates for increased system complexity, cost, and power consumptions [1]. Among the many solutions adopting multiple–antennas at either the transmitter, the receiver, or both, Spatial Modulation (SM) is a novel and recently proposed transmission technique for Multiple-Input-Multiple-Output (MIMO) wireless systems, which can offer good data rates and error performance with a moderately low system complexity [2]–[4].

SM has been conceived with a twofold objective [4]: i) reduce the hardware and computational complexity of conventional spatial multiplexing concepts for MIMO systems, and ii) guarantee a multiplexing gain with respect to conventional single–antenna systems. This is achieved by introducing the joint coding and modulation mechanism called *transmit–antenna index coded modulation*, which has two main features: 1) only one transmit–antenna is activated for data transmission at any signaling time instance, and 2) the spatial position of each transmit–antenna (known as *spatial constellation diagram* [4], [5]) is used as an additional source of information. In particular, 1) results in a significant reduction in transmitter and receiver complexity. This is because neither multiple Radio Frequency (RF) units at the transmitter, nor complicated interference cancelation mechanisms at the receiver are required. While this might result in a non–negligible reduction of the achievable data rate, however, 2) allows us to re–store the multiplexing gain potentially offered by multiple–antenna systems even though a single transmit–antenna is active for data transmission at any given time instance. In particular, i) if compared to single–antenna systems, SM offers, without any bandwidth expansion, a multiplexing gain that increases logarithmically with the number of antennas at the transmitter; while ii) if compared to MIMO spatial multiplexing systems, SM offers, with a single RF chain at the transmitter, a multiplexing gain that, although increases only logarithmically with the number of transmit–antennas, is independent of the number of receive–antennas, thus making this technology well suited for downlink transmissions. Furthermore, SM offers an intrinsic flexibility that allows us to choose, almost independently, the number of transmit–antennas and the modulation order to meet the desired data rate. Unlike other MIMO techniques it does not place a limiting constraint on the number of receive–antennas. This degree of freedom can be exploited to adjust the diversity gain and the error performance of the system [4], [5]. Further details about advantages and disadvantages of SM can be found in [4]–[6] and are here omitted due to space constraints.

Due to its potential benefits, several papers are now available in the literature, which are aimed at understanding the performance of SM–MIMO schemes and proposing new solutions with improved performance and flexibility. Some notable results can be found in [4]–[15] and references therein. From these research efforts, we have gained important information about the relative performance of SM with respect to other MIMO systems (see, *e.g.*, [4], [5], [8]). We know the optimal detectors with and without channel state information (see, *e.g.*, [5], [6], [12]), and we have a thorough understanding of the performance of SM over fading channels from which important insights for system optimization can be derived (see, *e.g.*, [11]–[15]).

However, all the contributions available so far have a common limitation: they are useful only for point–to–point communication systems, *i.e.*, the single–user scenario. Since,

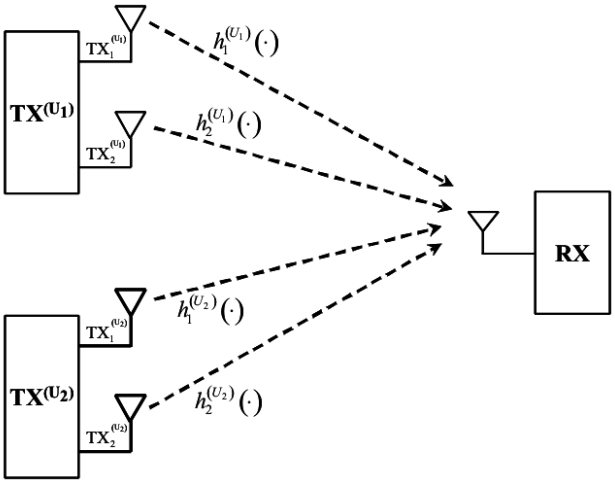

Fig. 1. System model: multiple–access channel with 2 transmitters and 1 receiver.

it is well–known that the performance of many wireless communication networks is interference limited (see, *e.g.*, [16] and references therein), due to the mutual interference arising from simultaneously transmitting users, the main objective of this paper is to study the performance and assess the suitability for communication of SM over multiple–access fading channels. Two receiver designs are considered: i) a single–user detector, and ii) a multi–user detector. Our analytical frameworks and numerical simulations show that the former detector cannot guarantee good performance (*i.e.*, a low Average Bit Error Probability – ABEP) for arbitrary channel conditions, while the latter detector can enable data transmission with performance very close to the point–to–point communication system. The main contribution of this paper is to show that SM with multi–user detection can indeed be adopted for enabling data transmission over multiple–access fading channels.

The remainder of this paper is organized as follows. In Section II, system and channel models are introduced. In Section III and Section IV, the performance of SM over multiple–access fading channels with a single– and a multi–user detector is analyzed, respectively. In Section V, numerical and simulation results are shown to substantiate the accuracy of the analytical framework and validate our claims. Finally, Section VI concludes the paper.

II. System Model

The system model analyzed in this paper is sketched in Fig. 1. Due to the analytical complexity of computing the performance of SM over fading channels even for the single–user system setup (see, *e.g.*, [11], [14]), we resort to some assumptions in this paper, which we emphasize here do not invalidate the generality of the conclusions drawn for the multiple–access channel. In particular, the following assumptions are considered. i) We restrict the analysis to the so–called Space Shift Keying (SSK) modulation scheme, which is a low–complexity implementation of SM trading–off data rate for complexity [5]. In SSK modulation, there is only one information carrying unit and the data stream is encoded only on the spatial constellation diagram [11]. ii) We consider the basic multiple–access channel with only two transmitters and one receiver. iii) Each transmitter is equipped with an antenna array with $N_t = 2$ transmit–antennas and the single receiver is equipped with $N_r = 1$ receive–antennas. This is the simplest configuration required to adopt the SSK modulation scheme. iv) Similar to previous research contributions [2]–[15], and for analytical tractability, we assume that a pure sinusoidal waveform is transmitted for each signaling interval. By assuming perfect time–synchronization at the receiver, this allows us to neglect the effect of the propagation delays in our analysis since each delay would result in an equivalent phase shift of the sinusoidal waveform, which can be embedded into the complex gain of the wireless channel (see Section II-B). This might be seen as equivalent to considering the synchronous multiple–access reference scenario [17].

According to [4], [5], SSK modulation works as follows: i) each transmitter encodes blocks of $\log_2(N_t)$ data bits into the index of a single transmit–antenna (*i.e.*, antenna–index coded modulation), which is switched on for data transmission while all other antennas are kept silent, and ii) the receiver solves a hypothesis detection problem to estimate, for each transmitter, the transmit–antenna that is not idle, which results in the estimation of the unique sequence of bits emitted by each encoder. Throughout this paper, the unique block of bits encoded into the index of the i–th transmit–antenna is called "message" and is denoted by $m_i^{(U_1)}$ and $m_i^{(U_2)}$ with $i = 1, 2, \ldots, N_t$ for user U_1 and user U_2, respectively. The N_t messages are assumed to be emitted with equal probability by each encoder. Moreover, the related transmitted signal is denoted by $s_i^{(U_1)}(\cdot)$ and $s_i^{(U_2)}(\cdot)$ with $i = 1, 2, \ldots, N_t$ for user U_1 and user U_2, respectively. It is implicitly assumed in this notation that, if $m_i^{(U_1)}$ is transmitted, the analog signal $s_i^{(U_1)}(\cdot)$ is emitted by the i–th transmit–antenna while all other transmit–antennas radiate no power. A similar assumption is considered for user U_2 as well.

Interference Channel: In this paper, we are mainly interested in the scenario where the single receiver in Fig. 1 has to decode the messages sent by both users. However, another scenario of practical interest is represented by the setup with two transmitters ($\mathrm{TX}^{(U_1)}$ and $\mathrm{TX}^{(U_2)}$) and two receivers ($\mathrm{RX}^{(U_1)}$ and $\mathrm{RX}^{(U_2)}$), where $\mathrm{TX}^{(U_1)}$ has a message only for $\mathrm{RX}^{(U_1)}$, and $\mathrm{TX}^{(U_2)}$ has a message only for $\mathrm{RX}^{(U_2)}$. This setup is called *interference channel* [18]. In this paper, we show that for this latter scenario even the single–user detector, for some fading channel conditions, might be sufficient to allow each receiver to adequately decode its intended message.

A. Notation

Let us briefly summarize the main notation used throughout this paper. i) We adopt a complex–envelope signal representation. ii) $j = \sqrt{-1}$ is the imaginary unit. iii) $(x \otimes y)(t) = \int_{-\infty}^{+\infty} x(\xi)\, y(t-\xi)\, d\xi$ is the convolution of signals $x(\cdot)$ and $y(\cdot)$. iv) $(\cdot)^*$ denotes complex–conjugate. v) $|\cdot|^2$ denotes square absolute value. vi) $\mathrm{E}\{\cdot\}$ is the expectation operator. vii) $\mathrm{Re}\{\cdot\}$ denotes the real part operator. viii) $\Pr\{\cdot\}$ means probability. ix) $\delta(\cdot)$ is the Dirac delta function. x) $Q(x) = \left(1/\sqrt{2\pi}\right) \int_x^{+\infty} \exp\left(-t^2/2\right) dt$ is the Q–function. xi) $\hat{m}^{(U_1)}$ and $\hat{m}^{(U_2)}$ denote the messages estimated at the receiver for user U_1 and user U_2, respectively. xii) E_m is the energy transmitted by each antenna that emits a non–zero signal. xiii) T_m denotes the signaling interval for each transmitted information message. xiv) The complex Additive White Gaussian Noise (AWGN) at the receiver input is denoted by $n(\cdot)$, and its real and imaginary parts are assumed to have a double–sided power spectral density equal to N_0. xv) $G \sim N\left(\mu_G, \sigma_G^2\right)$ is

$$\mathrm{ABEP}^{(U_1)} = \frac{1}{2}\mathrm{E}\left\{ Q\left(\sqrt{\frac{E_m^2}{4E_m N_0 + 4E_m^2 \left(\sigma_1^{(U_2)}\right)^2} \left|\alpha_2^{(U_1)} - \alpha_1^{(U_1)}\right|^2} \right) \right\} + \frac{1}{2}\mathrm{E}\left\{ Q\left(\sqrt{\frac{E_m^2}{4E_m N_0 + 4E_m^2 \left(\sigma_2^{(U_2)}\right)^2} \left|\alpha_2^{(U_1)} - \alpha_1^{(U_1)}\right|^2} \right) \right\}$$
$$= \frac{1}{2} - \frac{1}{4}\sqrt{\frac{E_m^2\left[\left(\sigma_1^{(U_1)}\right)^2 + \left(\sigma_2^{(U_1)}\right)^2\right]}{4E_m N_0 + 4E_m^2\left(\sigma_1^{(U_2)}\right)^2 + E_m^2\left[\left(\sigma_1^{(U_1)}\right)^2 + \left(\sigma_2^{(U_1)}\right)^2\right]}} - \frac{1}{4}\sqrt{\frac{E_m^2\left[\left(\sigma_1^{(U_1)}\right)^2 + \left(\sigma_2^{(U_1)}\right)^2\right]}{4E_m N_0 + 4E_m^2\left(\sigma_2^{(U_2)}\right)^2 + E_m^2\left[\left(\sigma_1^{(U_1)}\right)^2 + \left(\sigma_2^{(U_1)}\right)^2\right]}} \quad (5)$$

a Gaussian distributed Random Variable (RV) with mean μ_G and standard deviation σ_G. xvi) For ease of notation, we set $\bar{\gamma}{=}E_m/(4N_0)$.

B. Channel Model

We consider a frequency–flat slowly–varying fading channel model, with fading envelopes distributed according to a Rayleigh distribution [19]. Moreover, we assume the fading gains not to be necessarily identically distributed, but, for analytical tractability, uncorrelated fading is considered. In particular ($i = 1, 2, \ldots, N_t$):

- $h_i^{(U_1)}(t) = \beta_i^{(U_1)} \exp\left(j\varphi_i^{(U_1)}\right) \delta\left(t - \tau_i^{(U_1)}\right)$ and $h_i^{(U_2)}(t) = \beta_i^{(U_2)} \exp\left(j\varphi_i^{(U_2)}\right) \delta\left(t - \tau_i^{(U_2)}\right)$ are the channel impulse responses from the transmit–antennas $\mathrm{TX}_i^{(U_1)}$ and $\mathrm{TX}_i^{(U_2)}$ to the single receive–antenna for user U_1 and user U_2, respectively. Furthermore, $\beta_i^{(U_1)}$, $\varphi_i^{(U_1)}$, $\tau_i^{(U_1)}$, and $\beta_i^{(U_2)}$, $\varphi_i^{(U_2)}$, $\tau_i^{(U_2)}$ denote gain, phase, and delay of the related wireless link. Finally, $\alpha_i^{(U_1)} = \beta_i^{(U_1)} \exp\left(j\varphi_i^{(U_1)}\right)$ and $\alpha_i^{(U_2)} = \beta_i^{(U_2)} \exp\left(j\varphi_i^{(U_2)}\right)$ denote the complex channel gains.
- According to a Rayleigh fading channel model, the complex channel gains for user U_1, $\alpha_i^{(U_1)}$, reduce to $\alpha_i^{(U_1)} = \alpha_i^{(U_1),R} + j\alpha_i^{(U_1),I}$, where $\alpha_i^{(U_1),R} \sim N\left(0, \left(\sigma_i^{(U_1)}\right)^2\right)$ and $\alpha_i^{(U_1),I} \sim N\left(0, \left(\sigma_i^{(U_1)}\right)^2\right)$. Moreover, the fading gains over all wireless links are assumed to be independent from each other. A similar notation is used for user U_2.
- According to the assumptions in Section II, the propagation delays $\tau_i^{(U_1)}$ and $\tau_i^{(U_2)}$ are neglected in the reminder of this paper.

III. Single–User Detector

Let us consider that the receiver uses a single–user detector to estimate the messages transmitted by each user. Also, let us assume that the receiver has perfect Channel State Information (CSI) for each user. For a single–user detector, the receiver exploits only the CSI of the user it intends to decode. Without loss of generality, we study the performance of the system when U_1 is the intended user. Similar considerations can be made for user U_2. Finally, we denote by $m_{l_1}^{(U_1)} \in \left\{m_1^{(U_1)}, m_2^{(U_1)}\right\}$ and $m_{l_2}^{(U_2)} \in \left\{m_1^{(U_2)}, m_2^{(U_2)}\right\}$ the messages actually transmitted by user U_1 and user U_2, respectively.

A. Maximum–Likelihood (ML) Detector

Accordingly, the received signal, $r(\cdot)$, can be written as follows:

$$r(t) = \tilde{s}_{l_1}^{(U_1)}(t) + \tilde{s}_{l_2}^{(U_2)}(t) + n(t) \quad (1)$$

where $s_{l_1}^{(U_1)}(t) = s_{l_2}^{(U_2)}(t) = \sqrt{E_m}$ in $t \in [0, T_m]$, and:

$$\begin{cases} \tilde{s}_{l_1}^{(U_1)}(t) = \left(s_{l_1}^{(U_1)} \otimes h_{l_1}^{(U_1)}\right)(t) = \beta_{l_1}^{(U_1)} \exp\left(j\varphi_{l_1}^{(U_1)}\right) s_{l_1}^{(U_1)}(t) \\ \tilde{s}_{l_2}^{(U_2)}(t) = \left(s_{l_2}^{(U_2)} \otimes h_{l_2}^{(U_2)}\right)(t) = \beta_{l_2}^{(U_2)} \exp\left(j\varphi_{l_2}^{(U_2)}\right) s_{l_2}^{(U_2)}(t) \end{cases} \quad (2)$$

The ML–optimum single–user detector for user U_1 can be written as follows [17], [20]:

$$\hat{m}^{(U_1)} = \begin{cases} m_1^{(U_1)} & \text{if } D_1^{(U_1)} \geq D_2^{(U_1)} \\ m_2^{(U_1)} & \text{if } D_2^{(U_1)} < D_1^{(U_1)} \end{cases} \quad (3)$$

where we have defined:

$$\begin{cases} D_1^{(U_1)} = \mathrm{Re}\left\{\int_{T_m} r(t)\left(\tilde{s}_1^{(U_1)}(t)\right)^* dt\right\} - \frac{E_1^{(U_1)}}{2} \\ D_2^{(U_1)} = \mathrm{Re}\left\{\int_{T_m} r(t)\left(\tilde{s}_2^{(U_1)}(t)\right)^* dt\right\} - \frac{E_2^{(U_1)}}{2} \end{cases} \quad (4)$$

with $E_1^{(U_1)} = \int_{T_m} \tilde{s}_1^{(U_1)}(t)\left(\tilde{s}_1^{(U_1)}(t)\right)^* dt$ and $E_2^{(U_1)} = \int_{T_m} \tilde{s}_2^{(U_1)}(t)\left(\tilde{s}_2^{(U_1)}(t)\right)^* dt$.

We note that, according to our notation, the detector in (3) is successful in detecting the message transmitted by user U_1 if and only if $\hat{m}^{(U_1)} = m_{l_1}^{(U_1)}$. A similar detector for user U_2 can be easily obtained, but, for the sake of conciseness, it is not reported here.

B. ABEP

The ABEP can be computed by using a methodology similar to, *e.g.*, [15]. Due to space constraints, we avoid here the details of the lengthly analytical derivation. However, in Section V we substantiate the accuracy of the analytical derivation via Monte Carlo simulations.

From (3), the ABEP of user U_1, $\mathrm{ABEP}^{(U_1)}$, is shown in (5) on top of this page. The ABEP of user U_2, $\mathrm{ABEP}^{(U_2)}$, can be obtained from (5) with the substitutions $U_1 \mapsto U_2$ and $U_2 \mapsto U_1$. Finally, we emphasize that the ABEP in (5) is exact and no approximations have been made to compute it.

C. Analysis for large Signal–to–Noise–Ratios (SNRs)

In order to get some insightful information about the system behavior, let us analyze the ABEP for large SNRs, *i.e.*, when $E_m/N_0 \gg 1$. For ease of notation and for the sake of conciseness, let us also assume $\sigma^{(U_1)} = \sigma_1^{(U_1)} = \sigma_2^{(U_1)}$ and $\sigma^{(U_2)} = \sigma_1^{(U_2)} = \sigma_2^{(U_2)}$. With these assumptions, the ABEP of user U_1 and user U_2 in (5) simplify as follows:

$$\begin{cases} \mathrm{ABEP}_{\mathrm{asymp}}^{(U_1)} = \frac{1}{2} - \frac{1}{2}\sqrt{\frac{\left(\sigma^{(U_1)}/\sigma^{(U_2)}\right)^2}{2 + \left(\sigma^{(U_1)}/\sigma^{(U_2)}\right)^2}} \\ \mathrm{ABEP}_{\mathrm{asymp}}^{(U_2)} = \frac{1}{2} - \frac{1}{2}\sqrt{\frac{\left(\sigma^{(U_2)}/\sigma^{(U_1)}\right)^2}{2 + \left(\sigma^{(U_2)}/\sigma^{(U_1)}\right)^2}} \end{cases} \quad (6)$$

The result in (6) clearly brings to our attention that the ABEP of both users depends on the power–imbalance ratio, *i.e.*, $\left(\sigma^{(U_1)}/\sigma^{(U_2)}\right)^2$, of the wireless links. Furthermore, we notice that a single–user detector cannot guarantee a low ABEP for both users since $\mathrm{ABEP}^{(U_1)}_{\mathrm{asymp}}$ and $\mathrm{ABEP}^{(U_2)}_{\mathrm{asymp}}$ have a discordant behavior with respect to the power–imbalance ratio $\left(\sigma^{(U_1)}/\sigma^{(U_2)}\right)^2$: the higher it is, the lower $\mathrm{ABEP}^{(U_1)}_{\mathrm{asymp}}$ is, but the higher $\mathrm{ABEP}^{(U_2)}_{\mathrm{asymp}}$ is. Further comments about this point are given in Section V, regarding both the multiple–access system setup shown in Fig. 1 and the interference channel setup described in Section II. Finally, (6) reveals that, for both users, a single–user detector cannot achieve arbitrary small error probabilities for arbitrary large values of E_m/N_0: the ABEP of both user shows an error floor that depends on the power–imbalance ratio $\left(\sigma^{(U_1)}/\sigma^{(U_2)}\right)^2$.

IV. Multi–User Detector

To overcome the intrinsic limitations highlighted in Section III-C for the single–user detector, in this section we focus our attention on the multi–user detector. In this case, the receiver in Fig. 1 jointly decodes the messages of transmitter $\mathrm{TX}^{(U_1)}$ and transmitter $\mathrm{TX}^{(U_2)}$ assuming perfect knowledge of CSI of both users.

A. ML Detector

Similar to Section III-A, the received signal, $r(\cdot)$, is given by (1) with the same signal definitions as in (2). However, the detector is different, and (3) and (4) no longer hold. The ML–optimum multi–user detector can be obtained from the general theory in [17], and, for SSK modulation, can be explicitly written as follows:

$$\left(\hat{m}^{(U_1)},\hat{m}^{(U_2)}\right)=\underset{\substack{\left(m_{i_1}^{(U_1)},m_{i_2}^{(U_2)}\right)\\ \text{for } i_1=1,2,\ldots,N_t\\ \text{and } i_2=1,2,\ldots,N_t}}{\arg\max}\left\{D_{i_1,i_2}^{(U_1),(U_2)}\right\} \tag{7}$$

where we have defined:

$$D_{i_1,i_2}^{(U_1),(U_2)}=\mathrm{Re}\left\{\int_{T_m} r(t)\left(\tilde{s}_{i_1,i_2}^{(U_1),(U_2)}(t)\right)^* dt\right\}-\frac{E_{i_1,i_2}^{(U_1),(U_2)}}{2} \tag{8}$$

with $E_{i_1,i_2}^{(U_1),(U_2)}=\int_{T_m}\tilde{s}_{i_1,i_2}^{(U_1),(U_2)}(t)\left(\tilde{s}_{i_1,i_2}^{(U_1),(U_2)}(t)\right)^* dt$, and $\tilde{s}_{i_1,i_2}^{(U_1),(U_2)}(t)=\tilde{s}_{i_1}^{(U_1)}(t)+\tilde{s}_{i_2}^{(U_2)}(t)$. Furthermore, the signals $\tilde{s}_i^{(U_1)}(\cdot)$ and $\tilde{s}_i^{(U_2)}(\cdot)$ can be found in (2).

Finally, we note that the detector in (7) is successful in detecting the messages transmitted by both user U_1 and user U_2, *i.e.*, $\left(\hat{m}^{(U_1)},\hat{m}^{(U_2)}\right)=\left(m_{l_1}^{(U_1)},m_{l_2}^{(U_2)}\right)$, if and only if $\max\limits_{(i_1,i_2)}\left\{D_{i_1,i_2}^{(U_1),(U_2)}\right\}=D_{l_1,l_2}^{(U_1),(U_2)}$ for $i_1=1,2,\ldots,N_t$ and $i_2=1,2,\ldots,N_t$.

B. ABEP

The computation of the ABEP of the multi–user detector in (7) is quite involving from the analytical point of view. So, in this paper we exploit union–bound methods and some heuristics to get simple but still accurate formulas. The methodology used to compute the ABEP encompasses two steps.

Step 1: We compute the error probability of detecting the pair of messages $\left(m_{l_1}^{(U_1)},m_{l_2}^{(U_2)}\right)$, *i.e.*, $\Pr\left\{\left(\hat{m}^{(U_1)},\hat{m}^{(U_2)}\right)\neq\left(m_{l_1}^{(U_1)},m_{l_2}^{(U_2)}\right)\right\}$. With a slight abuse of terminology, we define this probability of error as Average Symbol Error Probability (ASEP), $\mathrm{ASEP}^{(U_1),(U_2)}$. The ASEP can be computed from (7) by using union–bound methods [21].

By avoiding the details of the analytical derivation due to space constraints, the ASEP can be upper–bounded as follows:

$$\begin{aligned}\mathrm{ASEP}^{(U_1),(U_2)}&\leq\overline{\mathrm{ASEP}}^{(U_1),(U_2)}\\&=\frac{1}{N_t}\sum_{i_1=1}^{2N_t}\sum_{i_2=i_1+1}^{2N_t}\mathrm{PEP}\left(i_1,i_2\right)\end{aligned} \tag{9}$$

where $\mathrm{PEP}(\cdot,\cdot)$ is the Pairwise Error Probability (PEP) [21]. The PEPs in (9) can be obtained after lengthy analytical computations by using arguments similar to Section III-B. Due to space constraints, only the final result is reported in Appendix I without proof, which we intend to include in an extended journal version of this paper.

Step 2: We use heuristic arguments to obtain, from (9), an approximate expression of the ABEP for each user. Our considerations move from the fact that the ASEP in (9) will be mostly dominated by the user with the worst channel conditions. To understand this point, let us assume, for the sake of simplicity, a fading scenario with $\sigma^{(U_1)}=\sigma_1^{(U_1)}=\sigma_2^{(U_1)}$ and $\sigma^{(U_2)}=\sigma_1^{(U_2)}=\sigma_2^{(U_2)}$. Then, the ASEP in (9) is expected to be a good estimate of the ABEP of the user with the worst fading channel, *i.e.*, $\min\left\{\sigma^{(U_1)},\sigma^{(U_2)}\right\}$. So, our heuristic argument is that the ABEP of each user can be computed directly from (9) by simply replacing $\bar{\gamma}$ in (12)–(14) in Appendix I with the equivalent SNR seen, for each user, by the receiver.

In detail, by explicitly emphasizing that the ASEP in (9) depends on $\bar{\gamma}$, *i.e.*, $\mathrm{ASEP}^{(U_1),(U_2)}=\mathrm{ASEP}^{(U_1),(U_2)}(\bar{\gamma})$, the ABEP of user U_1 and user U_2 can be approximated as follows:

$$\begin{cases}\mathrm{ABEP}^{(U_1)}\cong\mathrm{ASEP}^{(U_1),(U_2)}\left(\bar{\gamma}^{(U_1)}\right)\\ \mathrm{ABEP}^{(U_2)}\cong\mathrm{ASEP}^{(U_1),(U_2)}\left(\bar{\gamma}^{(U_2)}\right)\end{cases} \tag{10}$$

where we have defined:

$$\begin{cases}\bar{\gamma}^{(U_1)}=\bar{\gamma}\left(\dfrac{\left(\sigma^{(U_1)}\right)^2+\left(\sigma^{(U_2)}\right)^2}{\left(\sigma^{(U_2)}\right)^2}\right)\\ \bar{\gamma}^{(U_2)}=\bar{\gamma}\left(\dfrac{\left(\sigma^{(U_1)}\right)^2+\left(\sigma^{(U_2)}\right)^2}{\left(\sigma^{(U_1)}\right)^2}\right)\end{cases} \tag{11}$$

If we compare the ABEP of the multi–user detector in (11) and the ABEP of the single–user detector in (5) and (6), we notice that in the former case there is no error probability floor for large SNRs, *i.e.*, when $E_m/N_0\gg 1$. This result illustrates the robustness of the multi–user detector with respect to the single–user one. The price to be paid, however, is the increased computational complexity, for a large number for users, of (7) with respect to (3) [17]. The accuracy of (11) is analyzed in Section V via Monte Carlo simulations.

V. Numerical and Simulation Results

In this section, we study the performance of SSK modulation over multiple–access fading channels, and aim at substantiating the analytical model and claims made in the above sections. The system setup for each simulation can be found for each figure in its caption. Furthermore, the performance of SSK modulation for the scenario shown in Fig. 1 is compared to the performance of a point–to–point

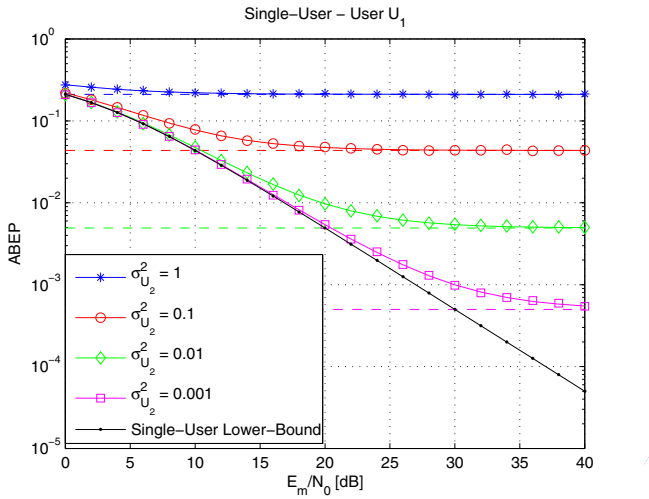

Fig. 2. ABEP against E_m/N_0 for user U_1 when a single–user detector is used ($\sigma^2_{U_1} = 1$). Markers denotes Monte Carlo simulations and solid lines the analytical model. Dashed lines represent the high–SNR asymptote of the analytical model (6).

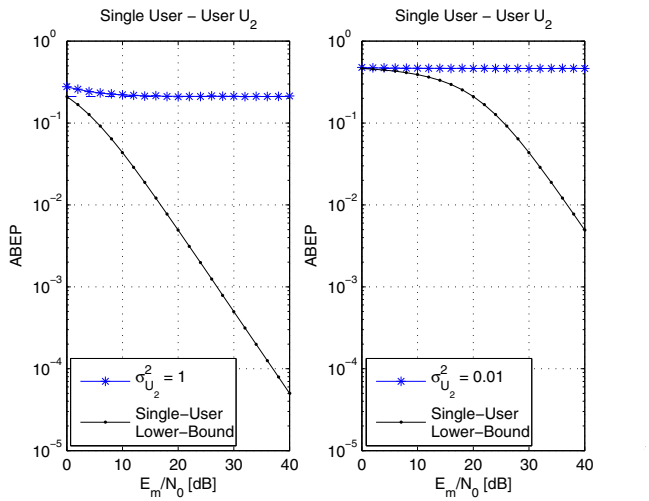

Fig. 3. ABEP against E_m/N_0 for user U_2 when a single–user detector is used ($\sigma^2_{U_1} = 1$). Markers denotes Monte Carlo simulations and solid lines the analytical model. Dashed lines represent the high–SNR asymptote of the analytical model (6).

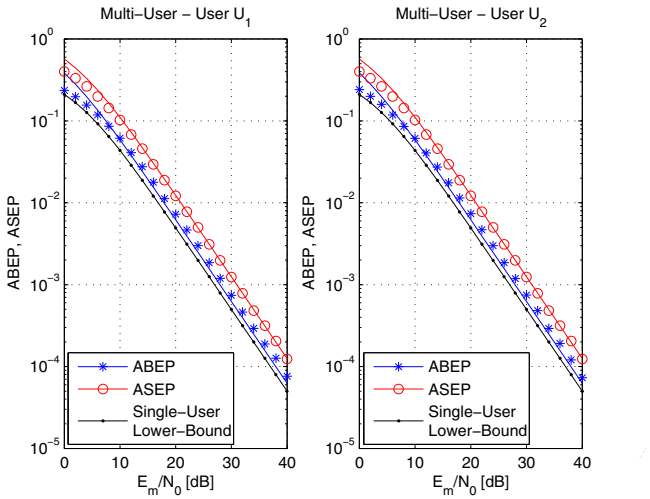

Fig. 4. ABEP and ASEP against E_m/N_0 for both users when a multi–user detector is used ($\sigma^2_{U_1} = 1$ and $\sigma^2_{U_2} = 1$). Markers denotes Monte Carlo simulations and solid lines the analytical model.

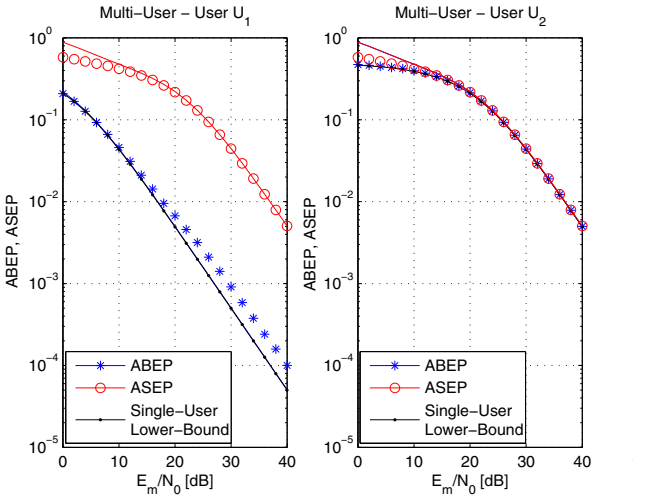

Fig. 5. ABEP and ASEP against E_m/N_0 for both users when a multi–user detector is used ($\sigma^2_{U_1} = 1$ and $\sigma^2_{U_2} = 0.01$). Markers denotes Monte Carlo simulations and solid lines the analytical model.

setup without multiple–access interference. Throughout this paper, the performance of this latter scenario is denoted by *single–user lower–bound*. The related analytical framework for Rayleigh fading channels can be found in [15].

In Fig. 2 and Fig. 3, we show the ABEP of the single–user detector in Section III for user U_1 and user U_2, respectively. The numerical examples shown in these figures confirm the claims of Section III: the single–user detector cannot guarantee good performance for both users, and only the user (user U_1 in Fig. 2 and Fig. 3) with the best channel conditions can achieve low error probabilities. In particular, only for high values of the power–imbalance ratio, $\left(\sigma^{(U_2)}/\sigma^{(U_1)}\right)^2 > 30\text{dB}$, user U_1 can achieve a good ABEP. Still in this case, though, an error probability floor can be observed as predicted by (6). Finally, we note that the analytical models developed in Section III-B agree very well with Monte Carlo simulations.

Let us now consider the *interference channel* setup introduced in Section II. In this case, each transmitter needs to deliver the information messages only to its intended receiver. The results in Fig. 2 and Fig. 3 show that user U_1 can successfully decode the message transmitted from $\text{TX}^{(U_1)}$ for high power–imbalance ratios. If a similar condition is verified, for user U_2 for the wireless links from transmitter $\text{TX}^{(U_2)}$ to the second receiver, then this receiver can also decode its intended message by simply using a single–user detector. This is allowed since each receiver sees different propagation channels from each transmitter, and so high values of the power–imbalance ratios can be simultaneously achieved for both of them. In other words, in the latter case SSK modulation exploits the deep fluctuations introduced by the path–loss and shadow–fading over the wireless links to differentiate the transmitted signals. This consideration resembles the key idea of designing opportunistic scheduling mechanisms using Cognitive Radios (CRs) (see, *e.g.*, [22], [23]).

In Fig. 4 and Fig. 5, we show the performance of the multi–user detector in Section IV. Unlike the single–user detector, we notice that in this case the receiver can decode the messages transmitted from both users, and for both of them it can achieve performance that is very close to the single–user lower–bound of each user. In Fig. 5 (left–hand side), we

notice that, for high SNRs, the multi–user detector is only slightly worse than the single–user lower–bound due to noise enhancement. The figures also confirm the accuracy of the proposed analytical model and approximation in Section IV-B. In particular, the approximation in (10) based on heuristics almost overlaps with the single–user lower–bound. This is especially true in Fig. 4. Finally the upper–bound in (9) matches very well with Monte Carlo simulations, and Fig. 5 confirms the claims in Section IV-B according to which (9) is mostly dominated by the user (U_2 in Fig. 5) experiencing the worst channel conditions.

VI. Conclusion

In this paper, we have studied the performance of SSK modulation over multiple–access fading channels. Two detectors have been proposed and their performance studied over uncorrelated Rayleigh fading channels. Numerical results have verified that the proposed analysis is quite accurate and that SSK modulation can be a suitable modulation and coding scheme for multiple–access fading channels, provided that a multi–user detector is used at the receiver.

Ongoing research is concerned with the analysis of a more general system setup with arbitrary number of users, transmitters, receivers, and channel conditions. Furthermore, recent results [24] have shown that, for the point–to–point scenario, the performance of SSK modulation can be improved with opportunistic power allocation methods. This possibility is currently being investigated for the multi–access scenario as well, with the main aim of developing distributed power allocation strategies based on, *e.g.*, game–theoretic methods.

Acknowledgment

We gratefully acknowledge support from the EPSRC (EP/G011788/1) for this work. Harald Haas acknowledges the Scottish Funding Council support of his position within the Edinburgh Research Partnership in Engineering and Mathematics between the University of Edinburgh and Heriot Watt University.

Appendix I
PEPs in (9)

The PEPs in (9) are as follows:

$$\begin{aligned}\mathrm{PEP}\,(1,2) = \mathrm{PEP}\,(3,4) &= Q\left(\sqrt{\bar{\gamma}\left|\alpha_2^{(U_2)} - \alpha_1^{(U_2)}\right|^2}\right) \\ &= \frac{1}{2} - \frac{1}{2}\sqrt{\frac{\bar{\gamma}\left[\left(\sigma_1^{(U_2)}\right)^2 + \left(\sigma_2^{(U_2)}\right)^2\right]}{1+\bar{\gamma}\left[\left(\sigma_1^{(U_2)}\right)^2 + \left(\sigma_2^{(U_2)}\right)^2\right]}}\end{aligned} \tag{12}$$

$$\begin{aligned}\mathrm{PEP}\,(1,3) = \mathrm{PEP}\,(2,4) &= Q\left(\sqrt{\bar{\gamma}\left|\alpha_2^{(U_1)} - \alpha_1^{(U_1)}\right|^2}\right) \\ &= \frac{1}{2} - \frac{1}{2}\sqrt{\frac{\bar{\gamma}\left[\left(\sigma_1^{(U_1)}\right)^2 + \left(\sigma_2^{(U_1)}\right)^2\right]}{1+\bar{\gamma}\left[\left(\sigma_1^{(U_1)}\right)^2 + \left(\sigma_2^{(U_1)}\right)^2\right]}}\end{aligned} \tag{13}$$

$$\begin{aligned}\mathrm{PEP}\,(1,4) = \mathrm{PEP}\,(2,3) &= Q\left(\sqrt{\bar{\gamma}\left|\left(\alpha_2^{(U_2)} - \alpha_1^{(U_2)}\right) - \left(\alpha_2^{(U_1)} - \alpha_1^{(U_1)}\right)\right|^2}\right) \\ &= \frac{1}{2} - \frac{1}{2}\sqrt{\frac{\bar{\gamma}\left(\sigma_{1,2}^{(U_1),(U_2)}\right)^2}{1+\bar{\gamma}\left(\sigma_{1,2}^{(U_1),(U_2)}\right)^2}}\end{aligned} \tag{14}$$

where $\sigma_{1,2}^{(U_1),(U_2)} = \sqrt{\sum_{i_1=1}^{N_t}\sum_{i_2=1}^{N_t}\left(\sigma_{i_2}^{\left(U_{i_1}\right)}\right)^2}$.

References

[1] J. Mietzner, R. Schober, L. Lampe, W. H. Gerstacker, and P. A. Höher, "Multiple–antenna techniques for wireless communications – A comprehensive literature survey", *IEEE Commun. Surveys Tuts.*, vol. 11, no. 2, pp. 87–105, 2nd quarter 2009.

[2] Y. Chau and S.–H. Yu, "Space modulation on wireless fading channels", *IEEE Veh. Technol. Conf. – Fall*, vol. 3, pp. 1668–1671, Oct. 2001.

[3] H. Haas, E. Costa, and E. Schultz, "Increasing spectral efficiency by data multiplexing using antennas arrays", *IEEE Int. Symp. Personal, Indoor, Mobile Radio Commun.*, vol. 2, pp. 610–613, Sept. 2002.

[4] R. Y. Mesleh, H. Haas, S. Sinanovic, C. W. Ahn, and S. Yun, "Spatial modulation", *IEEE Trans. Veh. Technol.*, vol. 57, no. 4, pp. 2228–2241, July 2008.

[5] J. Jeganathan, A. Ghrayeb, L. Szczecinski, and A. Ceron, "Space shift keying modulation for MIMO channels", *IEEE Trans. Wireless Commun.*, vol. 8, no. 7, pp. 3692–3703, July 2009.

[6] J. Jeganathan, A. Ghrayeb, and L. Szczecinski, "Spatial modulation: Optimal detection and performance analysis", *IEEE Commun. Lett.*, vol. 12, no. 8, pp. 545–547, Aug. 2008.

[7] J. Jeganathan, A. Ghrayeb, and L. Szczecinski, "Generalized space shift keying modulation for MIMO channels", *IEEE Int. Symp. Personal, Indoor, Mobile Radio Commun.*, pp. 1–5, Sept. 2008.

[8] R. Y. Mesleh, I. Stefan, H. Haas, and P. M. Grant, "On the performance of trellis coded spatial modulation", *Int. ITG Workshop on Smart Antennas*, pp. 235–241, Feb. 2009.

[9] A. Alshamali and B. Quza, "Performance of spatial modulation in correlated and uncorrelated Nakagami fading channel", *J. Commun.*, vol. 4, no. 3, pp. 170–174, Apr. 2009.

[10] S. U. Hwang, S. Jeon, S. Lee, and J. Seo, "Soft–output ML detector for spatial modulation OFDM systems", *IEICE Electronics Express*, vol. 6, no. 19, pp. 1426–1431, Oct. 2009.

[11] M. Di Renzo and H. Haas, "On the performance of space shift keying MIMO systems over correlated Rician fading channels", *IEEE Int. ITG Workshop on Smart Antennas*, pp. 72–79, Feb. 2010.

[12] M. Di Renzo and H. Haas, "Spatial modulation with partial–CSI at the receiver: Optimal detector and performance evaluation", *IEEE Sarnoff Symp.*, pp. 1–6, Apr. 2010.

[13] M. Di Renzo, R. Y. Mesleh, H. Haas, and P. Grant, "Upper bounds for the analysis of trellis coded spatial modulation over correlated fading channels", *IEEE Veh. Technol. Conf. – Spring*, May 2010, Taiwan, Taipei.

[14] M. Di Renzo and H. Haas, "On the performance of SSK modulation over correlated Nakagami–*m* fading channels", *IEEE Int. Conf. Commun.*, pp. 1–6, May 2010.

[15] M. Di Renzo and H. Haas, "Performance comparison of different spatial modulation schemes in correlated fading channels", *IEEE Int. Conf. Commun.*, pp. 1–6, May 2010.

[16] V. R. Cadambe and S. A. Jafar, "Reflections on interference alignment and the degrees of freedom for the K–user interference channel", *IEEE Inform. Theory Society Newsletter*, vol. 59, no. 4, pp. 5–9, Dec. 2009.

[17] S. Verdú, *Multiuser Detection*, Cambridge University Press, New York, 1998.

[18] V. R. Cadambe and S. A. Jafar, "Interference alignment and the degrees of freedom for the K–user interference channel", *IEEE Trans. Inform. Theory*, vol. 54, no. 8, pp. 3425–2441, Aug. 2008.

[19] M. K. Simon and M.–S. Alouini, *Digital Communication over Fading Channels: A Unified Approach to Performance Analysis*, John Wiley & Sons, Inc., 1st ed., 2000.

[20] H. L. Van Trees, *Detection, Estimation, and Modulation Theory, Part I: Detection, Estimation, and Linear Modulation Theory*, John Wiley & Sons, Inc. 2001, ISBNs: 0–471–09517–6.

[21] S. Haykin, *Communication Systems*, Wiley, 4th ed., 2000.

[22] M. Dohler, S. A. Ghorashi, M. Ghozzi, M. Arndt, F. Said, and A. H. Aghvami, "Opportunistic scheduling using cognitive radio", *Comptes Rendus Physique: Towards Reconfigurable and Cognitive Communications*, vol. 7, no. 7, pp. 805–815, Sept. 2006.

[23] M. Di Renzo, L. Imbriglio, F. Graziosi, and F. Santucci, "Distributed data fusion over correlated log–normal sensing and reporting channels: Application to cognitive radio networks", *IEEE Trans. Wireless Commun.*, vol. 8, no. 12, pp. 5813–5821, Dec. 2009.

[24] M. Di Renzo and H. Haas, "Improving the performance of space shift keying (SSK) modulation via opportunistic power allocation", *IEEE Commun. Lett.*, vol. 14, no. 6, pp. 500–502, June 2010.